Characterization of IQGAP1 Protein in Areas of Cell Retraction

By Michael Reimer, Bachelor of Science

A Thesis Submitted in Partial
Fulfillment of the Requirements
for the Degree of
Master of Science
in the field of Chemistry

Advisory Committee:

Joseph Schober, Chair

Kenneth Witt

Michael Shaw

Graduate School
Southern Illinois University Edwardsville
December, 2014

ABSTRACT

CHARACTERIZATION OF IQGAP1 PROTEIN IN AREAS OF CELL RETRACTION

by

MICHAEL REIMER

Chairperson: Professor Joseph Schober

IQGAP1 interacts with numerous binding partners through a calponin homology domain (CHD), a WW motif, IQ repeats, a Ras GAP related domain (GRD), and a conserved C-terminal (CT) domain. Among various biological and cellular functions, IQGAP1 plays a role in cell-matrix interactions and actin cytoskeleton dynamics in membrane ruffling and lamellipodium protrusion. Phosphorylation in the CT domain regulates intramolecular interaction and IQGAP1 cellular activity. In a recent study, we discovered that IQGAP1 surprisingly localizes to actively retracting edges, instead of protruding areas, in B16F10 mouse melanoma cells and some other cells types. In these current studies we examined localization of IQGAP1 mutants to retracting versus protruding areas in phorbol ester-stimulated B16F10 cells. Cells were co-transfected with GFP-IQGAP1 full length (GFP-IQGAP1-FL), as an internal control, and one of five Myc-tagged IQGAP1 constructs (FL, CA, ΔCHD, ΔGRD or ΔCT). The cotransfected cells were plated onto laminin for 30 minutes, stained with anti-Myc and anti-WAVE2 antibodies, and normalized fluorescence measurements were made in retracting and protruding areas. Retracting cell areas were defined as GFP-IQGAP1-FL positive and WAVE2 negative, while protruding cell areas were defined as GFP-IQGAP1-FL negative and WAVE2 positive. In retracting areas there were large decreases in both ΔGRD and ΔCT localization, a slight decrease in ΔCHD localization, and normal localization of the CA mutant. In areas of cell protrusion there were large increases in both ΔGRD and ΔCT localization, and normal localization of ΔCHD and CA

mutants. These results indicate that two domains, GRD and CT, are essential for normal localization of IQGAP1 to retracting cell areas. Furthermore, our results suggest a model in which IQGAP1 in the areas of cell retraction is in the open, phosphorylated, conformation. Additionally we investigated the knockdown of IQGAP1 in B16F10 cells by means of actin images. Cells were exposed to the lentil virus which contained short hairpin Ribonucleic acid (shRNA) that would silence IQGAP1. Two controls were used in the experiment, untransfected B16F10 cells and B16F10 cells which were exposed to the lentil virus without any shRNA. We found that the knockdown cells were in general much more compact and that they did not polarize. Surface stiffness was investigated in the effect it would have on B16F10 cells. Polyacrylamide gels were made and cross-linked using sulfo-SANPAH. Laminin was added to the cross-linked gels and B16F10 cells were placed on top of the laminin coated hydrogels. Investigation of the cells by means of actin images revealed that surface stiffness had an effect on cell morphology. The 1 kPa surfaces did not allow for spreading of the cells, while the surfaces greater than 100 kPa exhibited normal cell behavior.

ACKNOWLEDGEMENTS

I would like to first thank Dr. Schober for everything he has done for me. He has not only helped me grow as a scientist, but also as a person. I'm grateful for all of the advice and guidance he has given me. I would like to also thank Dr. Witt and Dr. Shaw for being members of my thesis committee. My friends definitely deserve acknowledgement for just being there when I needed them. Last, but certainly not least, I would like to thank my family. They have put up with me not only through my thesis writing, but my whole life.

TABLE OF CONTENTS

LIST OF FIGURES

CHAPTER I

INTRODUCTION

Cell Migration

What is cell migration

Cell migration is a biological function which is important in both development and maintenance for organisms. Proper cell migration is essential for many diverse biological functions such as embryogenesis, inflammatory response, and wound healing [1]. Cell migration is also involved in the migration of cancer cells, a process known as metastasis [2]. The fact that cell migration plays such a large role in these biological functions has led to much research into how cell migration is accomplished at a cellular level.

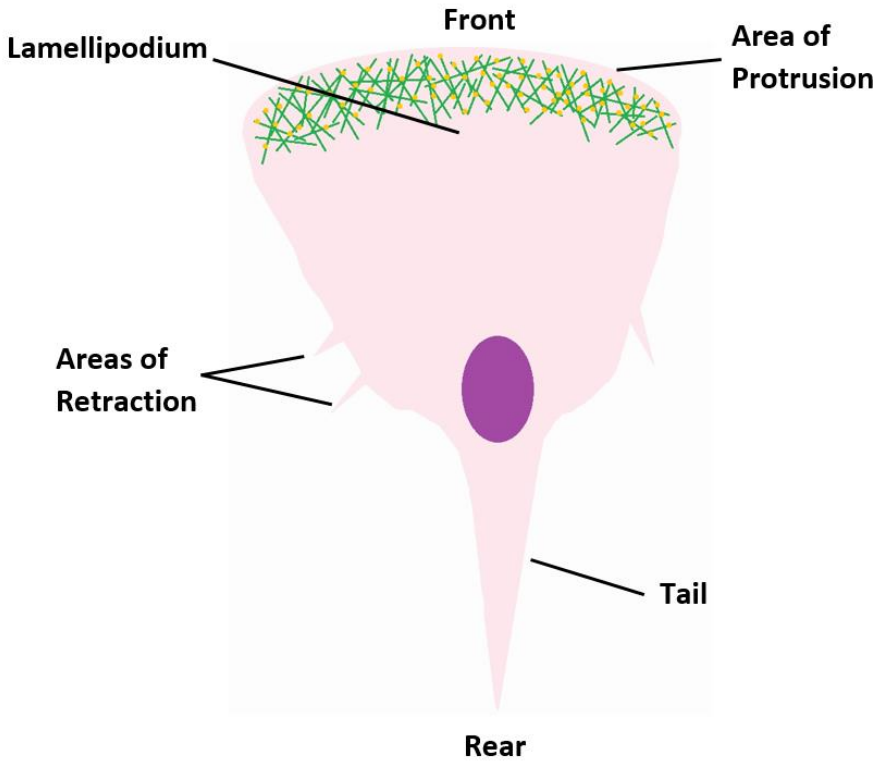

Figure 1. Polarized cell with IQGAP1 and actin. General cell shape for a polarized cell which has a rear and front. IQGAP1 is shown in orange at the leading edge of the cell where it is classically observed. Actin filaments are shown in green at the leading edge.

Research has shown that cells need to first generate an asymmetric morphology before they are able to migrate [1]. One such example of this asymmetric morphology is polarization of the cell. This polarized morphology is defined as a clear distinction between rear and front of the cell. An example of a cell exhibiting polarized morphology is shown above in Figure 1. At the top of the image there is a broad area known as the lamellipodium, this is the front of the polarized cell. At the bottom of the cell, the cell comes to a point. This point is known as the tail of the cell, and is the rear of the polarized cell. When the cell moves it pushes out at the lamellipodium and retracts at the tail, this is shown below in Figure 2. The first step in cell migration is extension, this is where the lamellipodium is pushed out further in front of the cell. Once the lamellipodium has extended the cell undergoes adhesion. Adhesion is the attachment of the extended lamellipodium to the surface it is residing on by means of adhesion sites. Once the extended lamellipodium has been adhered to the surface, the cell undergoes translocation. Translocation is when the cell uses intracellular forces to undergo movement of the entire cell in the direction of the new adhesion site. Once the cell has translocated the cell undergoes a process known as de-adhesion. This process entails the separation of the cell from the adhesion site which is located at the tail of the cell. This entire process of cell migration is performed by the cytoskeleton.

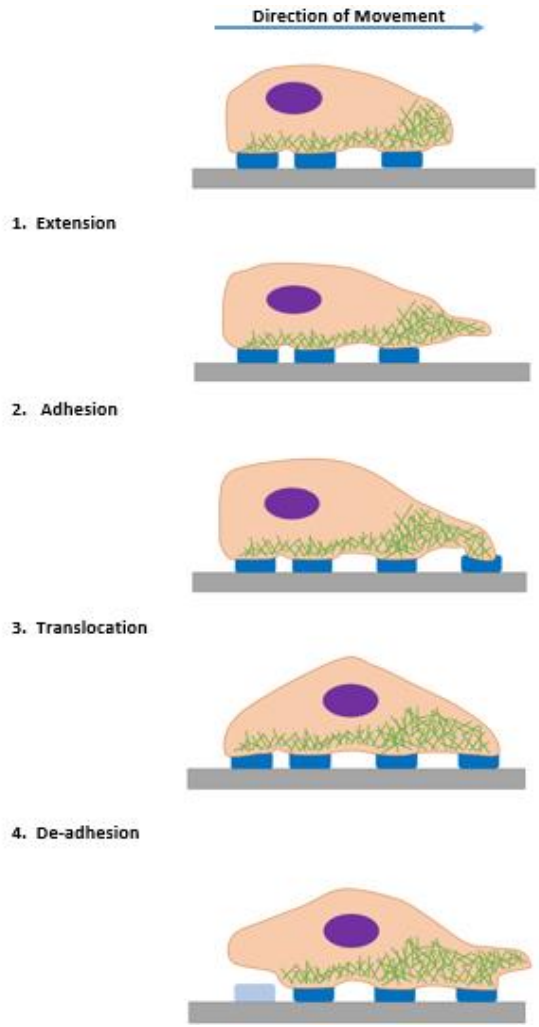

Figure 2. Process by which cell migration occurs. Extension occurs by the cell pushing the lamellipodium further out. The cell then performs adhesion by attaching the extended lamellipodium to the surface the cell resides on with adhesion sites. The entire cell then moves forward during the translocation step. Finally the cell detaches at the rear most adhesion site during the De-adhesion step.

Cell Cytoskeleton

The cytoskeleton is composed of three fibers: microfilaments, intermediate filaments, and microtubules. Microtubules are the thickest of the three fibers, and are important in intracellular transport as well as cell division. Intermediate filaments are much more stable than either microtubules or microfilaments. Intermediate filaments provide structural support for the cell and are located mainly around the nucleus. Microfilaments facilitate motion and are composed of proteins called actin.

Actin

Actin has two forms globular actin (G-actin) and filamentous actin (F-actin) as seen below in Figure 3. F-actin is responsible for polymerized actin microfilaments we see in cells. Adenosine tirphospate (ATP) binding to actin aids in the polymerization of G-actin to F-actin when compared to adenosine diphosphate (ADP) bound actin. Conversion of ATP bound F-actin to ADP bound F-actin by intrinsic ATPase activity facilitates a steric change by which F-actin dissociation to G-actin is now favored. Microfilaments are located throughout the cell, including the edges of the cell. While it is true that actin is the main driving force behind cell migration, without the structural support provided by the microtubules and intermediate filaments the cell would not maintain the proper shape for actin to work upon.

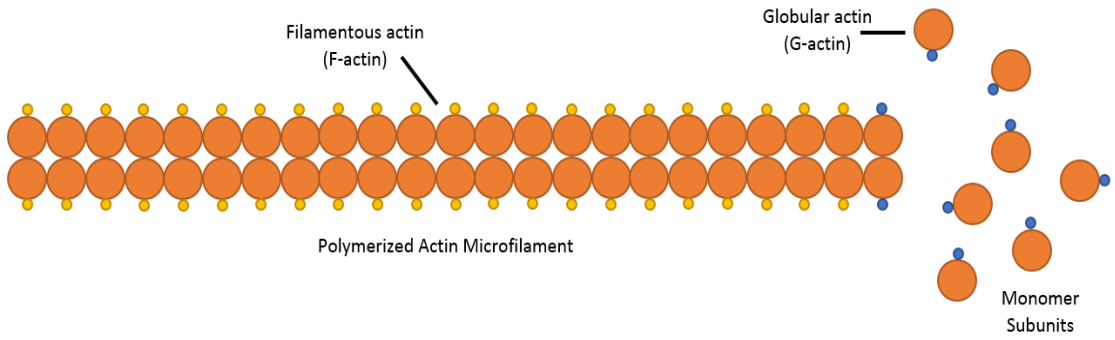

Figure 3. Microfilament structure and assembly. ATP bound actin polymerizes to form F-actin. Conversion of ATP to ADP by means of intrinsic ATPase activity results in a steric change in actin. This steric change results in F-actin dissociation to monomer subunits of G-actin.

IQGAP1

While the cytoskeleton is essential for cell migration it cannot do it without the use of many proteins which compose and help attach the cytoskeleton to adhesion sites. One of the many proteins involved in this process is IQGAP1. IQGAP1 has been shown to interact directly or as part of a complex with over ninety proteins to date [3]. Since IQGAP1

interacts with so many proteins it is thought to be involved in many cellular processes such as: regulation of cell motility, regulation of MAPK signaling, stimulation of branched actin filament assembly, regulation of cell proliferation, regulation of endothelial cell proliferation, and VEGF-induced angiogenesis among many others [3]. Figure 4 below shows an IQGAP1 schematic with binding partners listed for each of the domains. All of the binding partners listed have been shown to interact with IQGAP1 in vitro. Binding partners which are considered to be established binding partners are listed in black. These are binding partners which have numerous papers showing that they interact with IQGAP1. Binding partners in red are more recent binding partners which have only been identified since 2006.

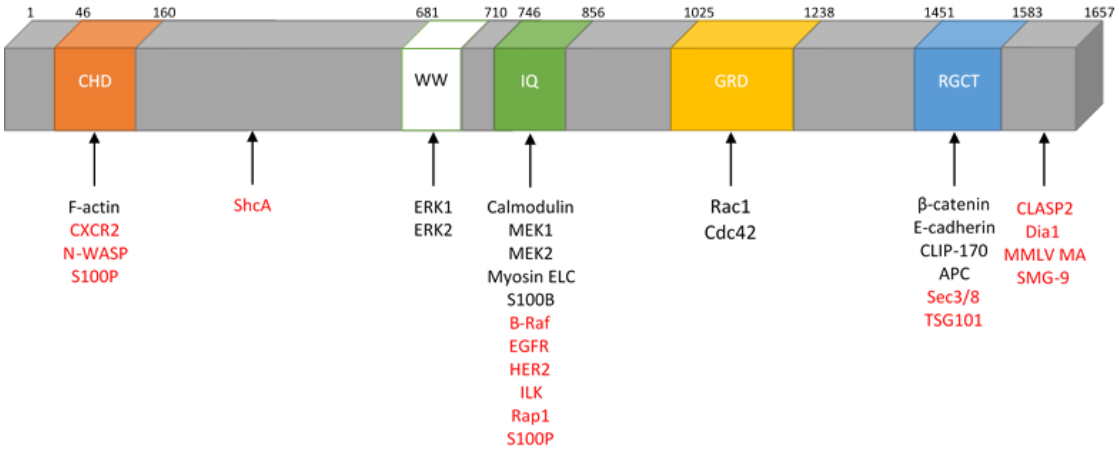

Figure 4. Schematic showing the domains of IQGAP1. All the domains of IQGAP1 are labeled in the schematic along with the first and last amino acid associated with the domain. Known binding partners of IQGAP1 are listed in black and recent potential binding partners are listed in red.

Classic role of IQGAP1 in cell migration

IQGAP1 has been shown to have several roles which would be important for proper cell migration. It has been shown to be important in the promotion of cross-linking of actin by means of direct binding as well as by interacting with N-WASP [4,5]. IQGAP1 has also been shown to regulate microtubule dynamics by interaction with CLIP-170 or APC [6,7].

IQGAP1 has additionally been shown to bind with E-cadherin directly and influence its function [8]. All of these interactions have been shown to occur at the leading edge of the cell. As Figure 1 above shows IQGAP1 has mainly been shown to localize at the lamellipodia, or leading edge of the cell.

Previous experimental data on IQGAP1

Looking at the research done on IQGAP1 our lab previously decided to use IQGAP1 as a marker for cell protrusion. When we performed the experiment however, we found that IQGAP1 was actually localizing to areas of retraction within the cell. We then decided to see if this was limited to the specific cell type we were using. As we can see in Figure 5 IQGAP1 is localizing to just behind areas of protrusion in both the A375 cells and NIH 3T3 cells. We also see in the CHO cells that it is actually localizing to areas of protrusion. We also can see in both the B16F10 and B16F1 cells that IQGAP1 localizes to areas of retraction. What we found was that IQGAP1 localization was cell type dependent and that it localized to areas of retraction in some cell lines, this can be seen below in Figure 5.

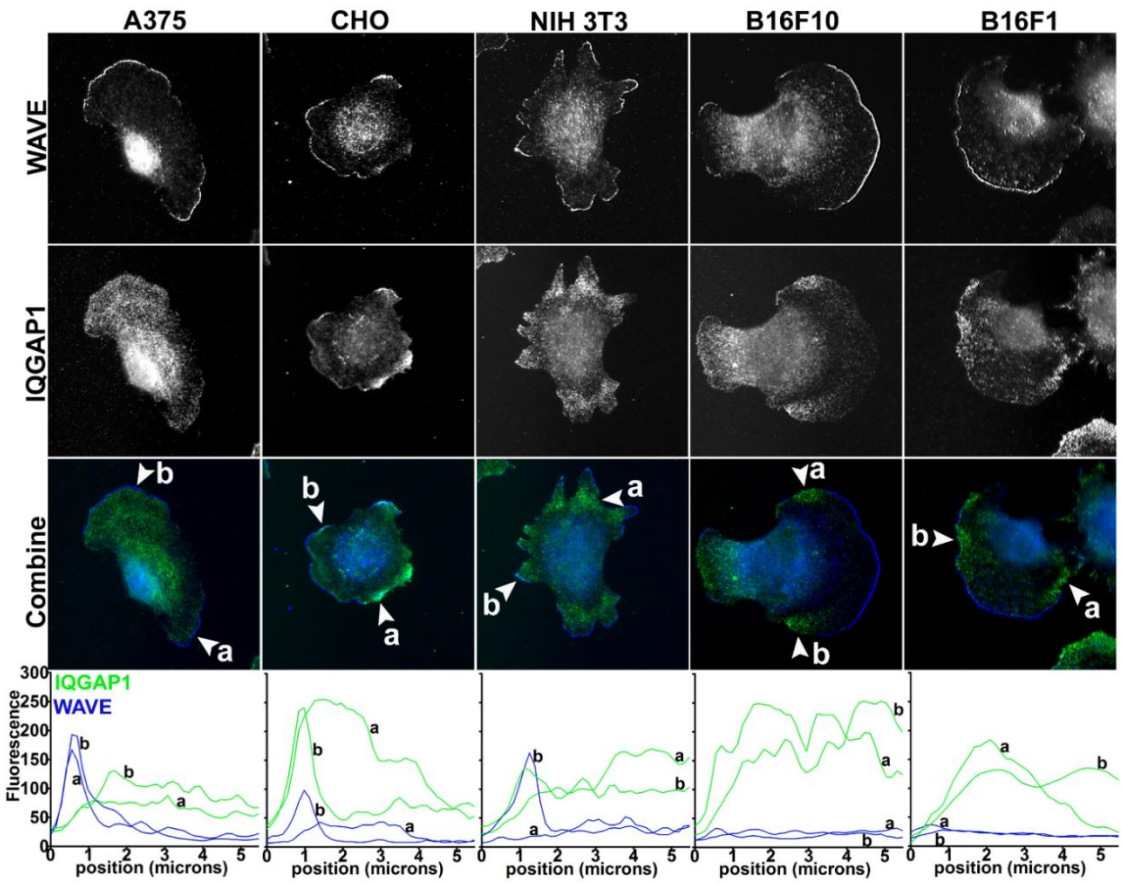

Figure 5. Subcellular localization of IQGAP1 and WAVE2 in various cell lines. Cell lines were stained with anti-IQGAP1 and anti-WAVE2 antibodies. Representative images for A375, CHO, NIH 3T3, B16F10, and B16F1 results are shown. The arrowheads in the color combined images (WAVE2 blue, IQGAP1 green) indicate the locations of linescans. The bottom of the figure shows the fluorescence intensity of the proteins that extend 5.5 microns into the cell at location a and b [11].

We then decided to further investigate localization of IQGAP1 by looking at GFP-IQGAP1 and mCherry-Arp3 localization in live B16F10 cells (Figure 6). Arp3 helps initiate actin filament branching in lamellipodia and is therefore a good marker for cell protrusion [9] What we can see in the image below is that over time, as the cell retracts, the fluorescence intensity for mCherry-Arp3 decreases as the fluorescence intensity for IQGAP1 increases. This is graphically demonstrated in the top plot of Figure 6. The bottom plot of Figure 6 shows that there is a correlation between cell edge retraction and the intensity of GFP-IQGAP1 fluorescence. The two experiments described provided us with strong evidence that

a novel role for IQGAP1 existed at areas of retraction. With this thought we set out to determine what domains in IQGAP1 were important for localization.

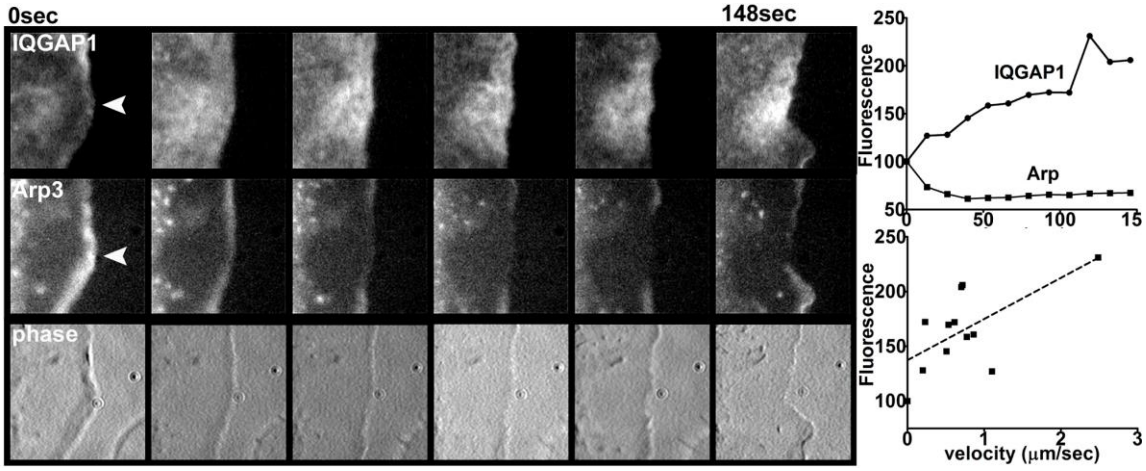

Figure 6. IQGAP1 and Arp3 fluorescence at cell edge retraction. A cotrasfection with GFP-IQGAP1 and mCherry-Arp3 was performed on B16F10 cells. The cells were then imaged on laminin over 148 seconds. The top graph is a plot of Arp3 and IQGAP1 fluorescence over time. The lower graph is a correlation of IQGAP1 fluorescence with cell edge retraction[11].

CHAPTER II

RESEARCH QUESTIONS

The question we were interested in finding the answer to was what domains are involved in the localization of IQGAP1 to areas of retraction with in the cell. We also wanted to explore if IQGAP1 was necessary for cell edge retraction. In order to attempt to find the answers to these questions we first obtained IQGAP1 mutants from Dr. Alfredo Caceres. We intended to use these mutants to help us determine how the loss of a domain would affect the localization of IQGAP1. Using this approach we would be able to determine if a single domain is responsible for the localization of IQGAP1 or if multiple domains are involved in the process. To attempt to determine if IQGAP1 is necessary for cell edge retraction we decided to perform a whole cell knockdown of IQGAP1 using RNA interference. The short hairpin RNA would be delivered into the cell using the lentivirus. In addition to the two research questions listed above we also wanted to know what impact surface stiffness had on the localization of IQGAP1. To investigate this we would use polyacrylamide gels of varying stiffnesses and observe where IQGAP1 localizes.

CHAPTER III

MATERIALS AND METHODS

Intracellular Localization of IQGAP1 Mutants

Cell lines

The cell line used for experiments was B16F10 which were purchased from American Type Culture Collection (Manassas, VA, USA). The cells were maintained in Dulbecco's Modified Eagle Medium (DMEM) which was supplemented with 10% fetal bovine serum (FBS) (Atlanta Biologicals, Lawrenceville, GA, USA) and antibiotics. Cell detachment was performed with by means of a trypsin/Ethylenediaminetetraacetic acid (EDTA) solution (Mediatech, Manassas, VA, USA).

Laminin coated coverslip preparation

Glass coverslips were coated with 30 µg/mL mouse laminin for 24 hours at 4 °C. The laminin coated coverslips were then placed into 35 mm diameter dishes which contained DMEM and freshly thawed 10% FBS.

Myc-tagged IQGAP1 mutants

Myc-tagged IQGAP1 mutants were obtained from Dr. Alfredo Caceras at Consejo Nacional de Investigaciones Científicas y Técnicas de Argentina. Figure 7 below shows the mutants and what domains are missing. The Myc-CA has two point mutations at residues 1441 and 1443. Myc-ΔCT has lost CT domain as well as the rest of the c-terminus. The Myc-ΔGRD has had the GRD domain removed, while the Myc-ΔCHD has lost the CHD domain as well as the n-terminus.

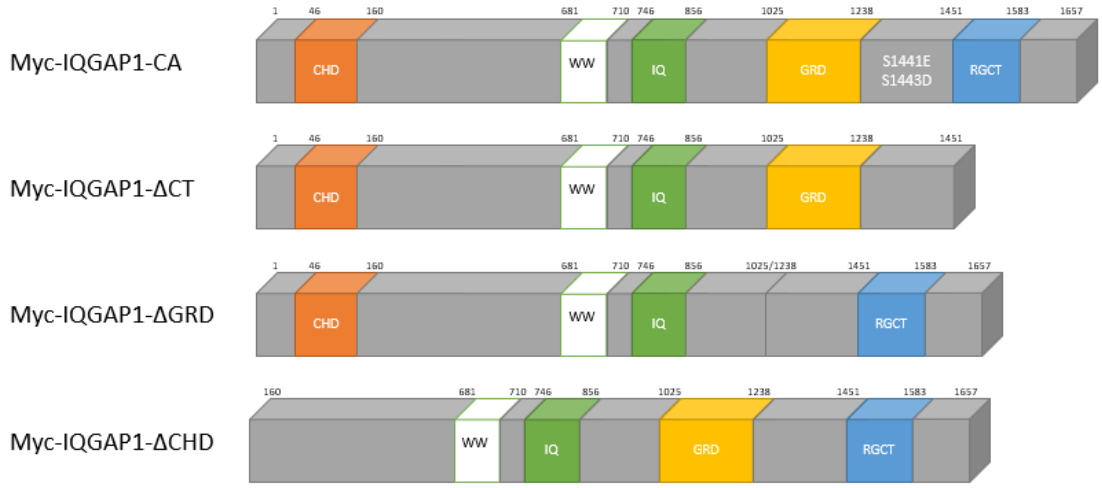

Figure 7. Schematics showing the IQGAP1 mutants. From top to bottom the mutants are: IQGAP1-CA, IQGAP1-ΔCT, IQGAP1-ΔCHD, and IQGAP1-ΔGRD.

Cell transfection

Transfection were performed by means of mixing Fugene 6 (Roche Diagnostics) with Myc-tagged IQGAP1 mutant plasmid as well as GFP-IQGAP1 plasmid in sterile DMEM. Transfection by means of Fugene 6 is shown below in Figure 8. The mixture was allowed to sit at 22 °C for 20 minutes. Each mixture was then added into separate 35 mm diameter dishes containing B16F10 cells. The dishes were then allowed to sit for 18 hours at 37 °C.

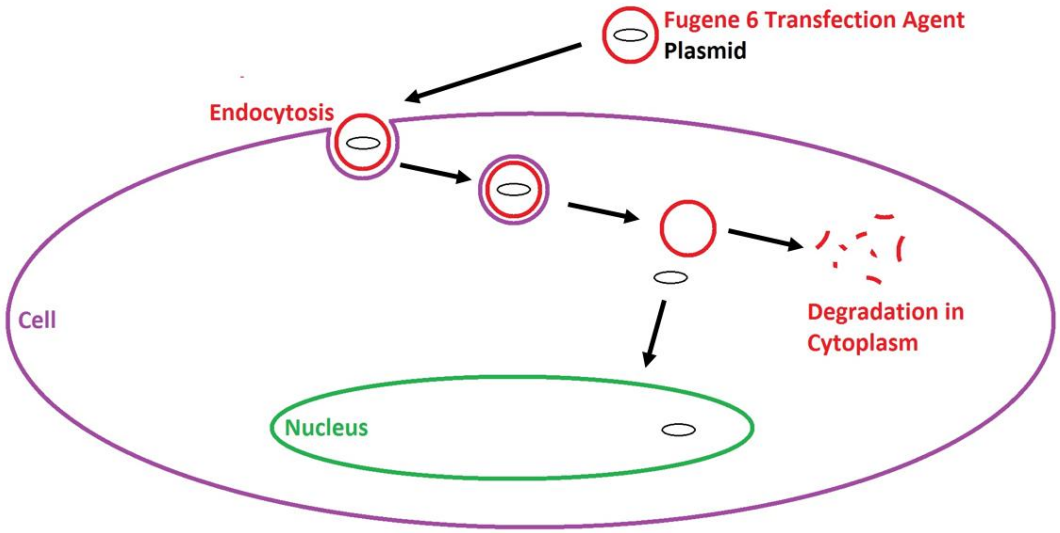

Figure 8. Transfection by means of Fugene 6 Transfection Agent. The agent first takes up the plasmid. The agent then enters the cell by means of endocytosis. The agent is then degraded in the cytoplasm thus releasing the plasmid. The plasmid then enters the nucleus.

Cell fixation and immunofluorescence staining

Transfected cells were placed onto laminin coated coverslips which were in a 35 mm diameter dishes which contained DMEM and freshly thawed 10% FBS. Cells were then incubated for 30-45 minutes at 37 °C and 5% CO_2. The coverslips were then fixed for 90 minutes at 22 °C in cytoskeleton-stabilizing buffer (80 mM PIPES, 2 mM EGTA, 3 mM $MgCl_2$, pH=6.9) with 4% paraformaldehyde and 0.1% Triton-X 100. Once fixation was complete the coverslips were washed in water and then placed into 2% bovine serum albumin (BSA) for 15 minutes for blocking. After blocking with BSA the coverslips were incubated with rabbit polyclonal anti-WAVE2 antibody (Santa Cruz, CA, USA) and mouse anti-Myc for 25 minutes at 37 °C. Coverslips were then washed with water and blocked with 0.2% BSA for 15 minutes. After the coverslips were blocked they were incubated with anti-rabbit-Alexa 647, anti-mouse-TriTc, and Hoechst stain for 25 minutes at 37 °C. After the secondary incubation the coverslips were washed in water and placed in PBS for 15 minutes at 22 °C. After the PBS wash the coverslips were wash once more with water and mounted onto glass slides using Aqua Poly/Mount (Polysciences, Warrington, PA, USA). Images were then acquired with a Leica DMIRE2 HC inverted epifluorescence microscope fitted with a 12-bit grayscale CCD camera.

Statistical analysis

Images of the immunofluorescence which were obtained were analyzed by means of Metamorph software. Cells were traced in the software and values for the whole cell fluorescence intensity of both GFP-IQGAP1 and Myc-IQGAP1 mutants and wild type were obtained. Three linescans were used both in areas of protrusion and retraction to obtain fluorescence intensity values in these areas of interest as well, this is seen below in Figure 9.

The linescan values were then divided by the whole cell values for their particular cell so that we could account for different levels of transfection and subsequent immunofluorescence staining in each cell. These ratios were then combined together to form a ratio of ratio value with the Myc-mutant value above the GFP-IQGAP1 value. We did this for both areas of protrusion and retraction.

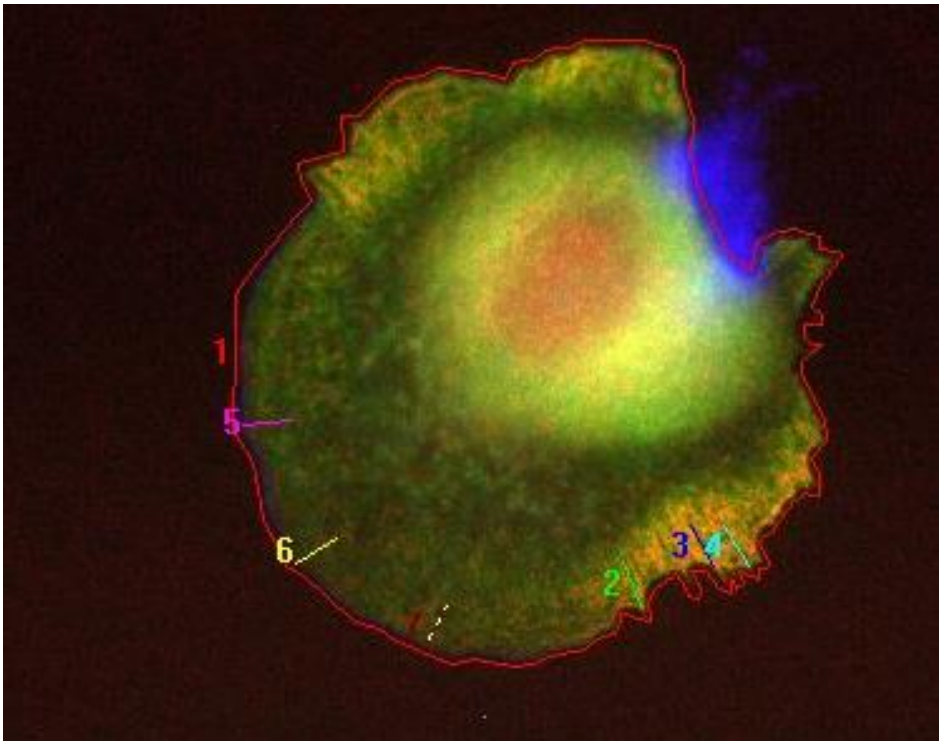

Figure 9. Raw image of a cell during analysis. Above is an image of a cell undergoing analysis in Metamorph software. The cell was first outlined as shown above by line 1. Three lines were then drawn in areas of retraction as seen by lines 2, 3, and 4. Three lines were then drawn in areas of protrusion as seen by lines 5, 6, and 7.

Knockdown with Short Hairpin RNA

Short hairpin RNA (shRNA) interference was used to create a line of B16F10 cells which had reduced levels of IQGAP1. This was achieved by using the lentivirus to insert shRNA into the cell to inhibit the production of IQGAP1. RNA interference works by inserting the shRNA into the cell. This process is shown below in Figure 10. A protein known as dicer then cuts the shRNA into a double stranded piece of RNA which is about 21-

23 nucleotides long. These cleaved strands are then incorporated into a complex known as pre-RISC. In this complex the double stranded RNA is separated into two single stranded RNAs. One of the single stranded RNAs in cleaved in two and dissociates while the other strand along with the rest of the pre-RISC complex is incorporated in a protein complex known as RISC. RISC uses the incorporated RNA to identify mRNA sequences which are complementary and then destroys them.

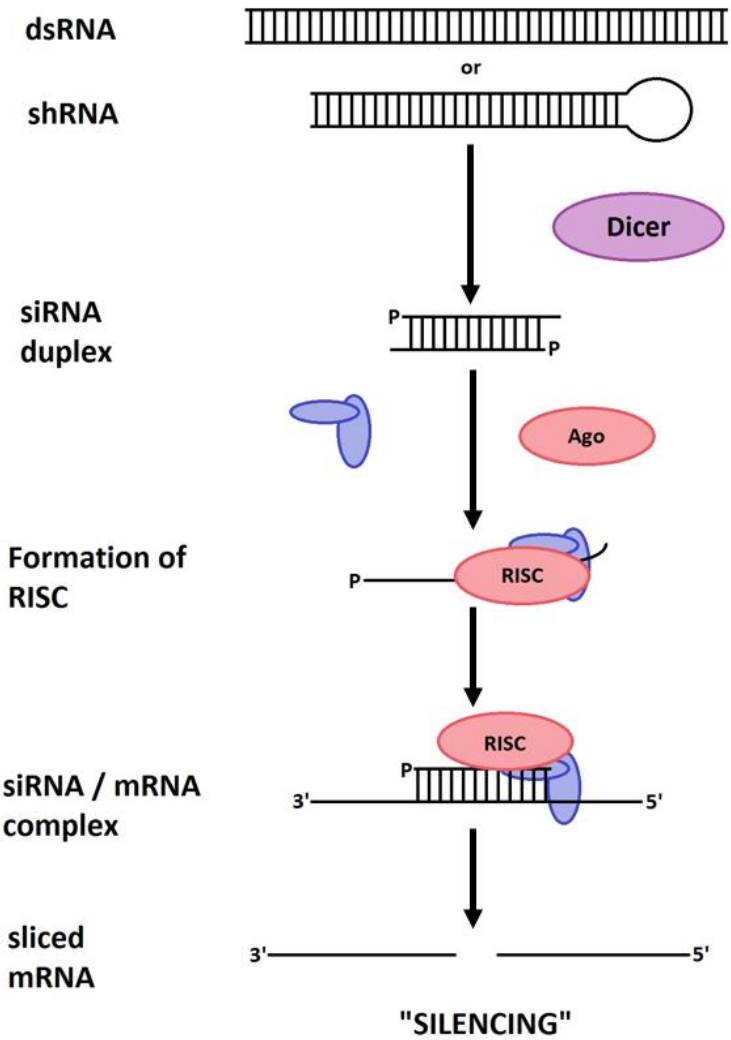

Figure 10. Silencing of gene expression by means of RNA interference. Double stranded RNA or short hairpin RNA is cut by dicer into short segments of RNA about 21-23 nucleotides long. These cleaved double stranded segments are then separated and one of the halves is incorporated into a complex known as RISC. RISC then uses the single stranded RNA segment to locate complementary segments in the cell and cleave them in half. This results in the silencing of the particular gene expression.

Polyacrylamide Hydrogel Preparation

Glass coverslips were coated with a bind-silane solution and incubated for 15 minutes at 22 °C. Once the incubation was finished the coverslips were left to air dry. In a fume hood, 80 µL of repel-silane was added in a dropwise manner to a glass slide and then spread using lens paper. Once the repel-silane was spread on the glass slide the solution was left to air dry in the hood. The hydrogel mixture was created by mixing 40% acrylamide, bis-acrylamide and ddH_2O for desired stiffness. 1 mL of the desired hydrogel mixture was placed in a 1.5 mL microcentrifuge tube and degassed for 10 minutes at 50 torr. Once the solution was degassed and both the repel-silane coated glass slide and bind-silane glass coverslip were dried 5µL of 10% APS and 0.5 µL of TEMED were quickly added to the degassed hydrogel solution. The resulting mixture of degassed hydrogel solution, APS, and TEMED was then quickly but gently inverted 12 times. 80 µL of the inverted solution was then quickly placed onto the repel-silane coated glass slide. The bind-silane coated coverslip was then placed with the bind-silane coated side face down on top of the drop. The solution was then allowed to polymerize at 22 °C for 60 minutes. After 60 minutes, the coverslip was carefully removed by means of a microspatula and place in a 35 mm-diameter dish which contained PBS. The coverslip was washed in the PBS for 15 minutes at 22 °C. The coverslips were then removed from the 35 mm-diameter dish and 300 µL of freshly made 500 µM sulfo-SANPAH which was diluted in water was quickly added to the hydrogels which were then placed under UV light for 5 minutes. It was important to prepare the sulfo-SANPAH solution, add the solution to the hydrogels, and place the hydrogels with solution into the UV light as quickly as possible because the crosslinking reaction of sulfo-SANPAH with the hydrogel has a competing reaction with the water used to dilute the sulfo-SANPAH.

This results in the sulfo-SANPAH losing the ability to act as a crosslinker if it is left in water for too long. Once the crosslinking is complete the coverslips were then washed with water to remove excess sulfo-SANPAH. Laminin was then added at 30 μg/mL onto the crosslinked coverslips and the coverslips were allowed to incubate at 22 °C for 30 minutes. After the incubation was complete the laminin coated coverslips were then washed in PBS to remove residual laminin. The washed coverslips were then placed into 35 mm-diameter dishes containing DMEM with 10% FBS and antibiotics. The dishes containing the laminin coated coverslips were then incubated for 30 minutes at 37 °C and 5% CO_2.

CHAPTER IV

RESULTS

Localization of Myc-Tagged IQGAP1 Mutants

In the following experiment for testing the Myc-tagged mutants we placed the transfected cells on to laminin coated coverslips and allowed them to attach and spread for 30 minutes. We then examined co-immunolocalization of GFP-IQGAP1 and Myc-WTFL mutants in B16F10 cells (Figure 11). Here we observed that localization of GFP-IQGAP1 and Myc-WTFL localized to the same areas of retraction. We also noted that the localization of both the GFP-IQGAP1 and Myc-WTFL was absent in the WAVE2 positive or protruding edges of the cell. The localization of both Myc-IQGAP1 and GFP-IQGAP1 to areas of retraction is proof that neither the GFP nor the Myc-tag are interfering with the localization

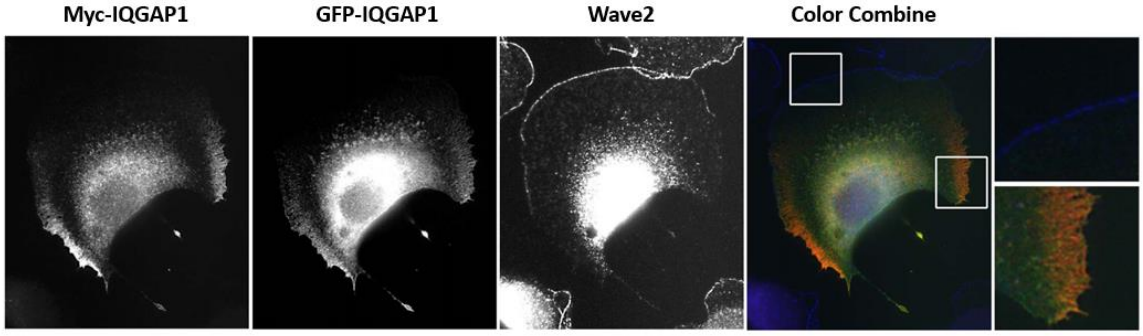

Figure 11. Subcellular localization of Myc-WTFL, GFP-IQGAP1, and WAVE2. B16F10 cells were double transfected with GFP-IQGAP1 and Myc-WTFL and were then stained with anti-Myc and anti-WAVE2 antibodies. The Myc-WTFL (red), GFP-IQGAP1 (green), and WAVE2 (blue) were combined and areas in retracting edges and protruding edges were enlarged.

of IQGAP1 in the B16F10 mouse melanoma cells.

We next looked at our constitutive active mutant of IQGAP1 which has two modifications to the protein, serine 1441 has been replaced with glutamate and serine 1443 has been replaced with aspartate. We observed that the Myc-CA also co-localized with the

GFP-IQGAP1 at areas of retraction (Figure 12). Additionally, we noticed that GFP-IQGAP1 and Myc-CA did not localize to WAVE2 positive areas. These results were expected since the Myc-CA was mimicking a phosphorylated IQGAP1 protein, and we expect to see the same localization of the Myc-CA as we did with the Myc-WTFL.

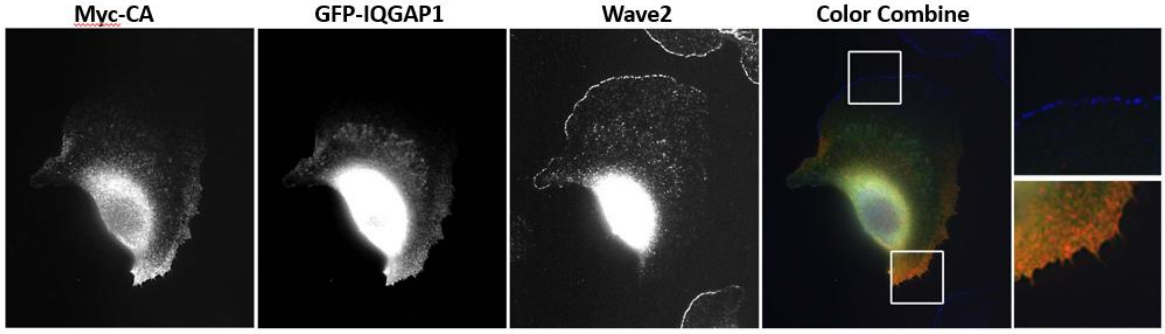

Figure 12. Subcellular localization of Myc-CA, GFP-IQGAP1, and WAVE2. B16F10 cells were double transfected with GFP-IQGAP1 and Myc-CA and were then stained with anti-Myc and anti-WAVE2 antibodies. The Myc-CA (red), GFP-IQGAP1 (green), and WAVE2 (blue) were combined and areas in retracting edges and protruding edges were enlarged.

Next we examined Myc-ΔCHD which is missing the N-terminus through the CHD domain of IQGAP1. As discussed earlier the CHD domain has been shown to cause IQGAP1 to localize to the protruding edge of various cell lines. We then examined Myc-ΔCHD in comparison to the GFP-IQGAP1 (Figure 13) and found that it localized to areas of retraction with GFP-IQGAP1 but not quite as well as the Myc-WTFL or Myc-CA. We also see that it does not localize to the WAVE2 positive areas of the cell. As is consistent with other studies we see that Myc-ΔCHD does not localize to areas of protrusion. This makes sense due to the fact that the CHD domain has been shown to be critical in that process.

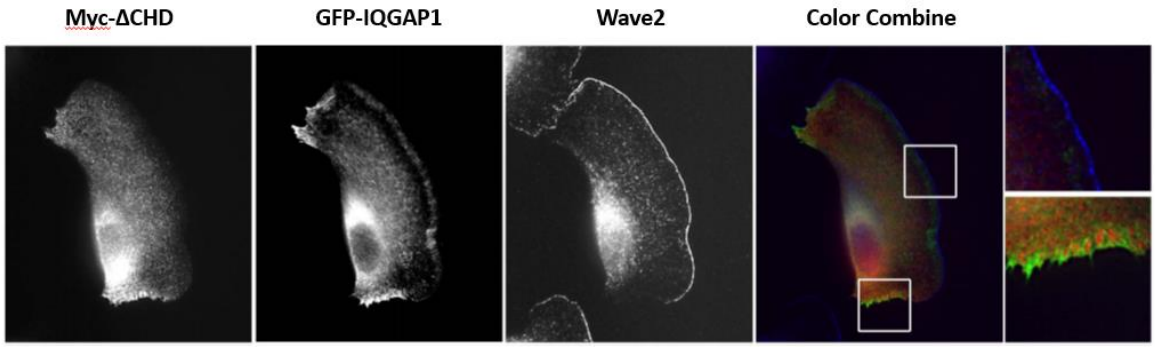

Figure 13. Subcellular localization of Myc-ΔCHD, GFP-IQGAP1, and WAVE2. B16F10 cells were double transfected with GFP-IQGAP1 and Myc-ΔCHD and were then stained with anti-Myc and anti-WAVE2 antibodies. The Myc-ΔCHD (red), GFP-IQGAP1 (green), and WAVE2 (blue) were combined and areas in retracting edges and protruding edges were enlarged.

When we examined the localization of GFP-IQGAP1 and Myc-ΔGRD (Figure 14) we saw that the two did not co-localize at all. In fact, we see the GFP-IQGAP1 in areas of retraction while we see the Myc-ΔGRD in WAVE2 positive areas of the cell. This provides evidence that in B16F10 mouse melanoma cells the GRD domain is important for the localization of IQGAP1 to areas of retraction.

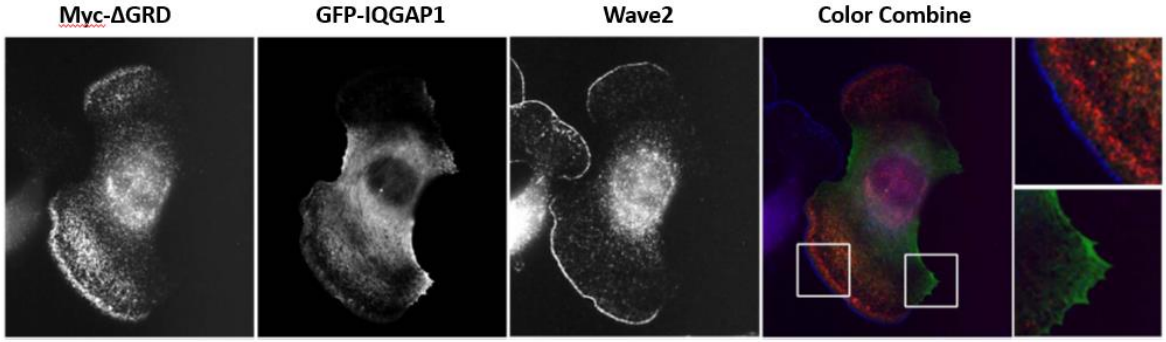

Figure 14. Subcellular localization of Myc-ΔGRD, GFP-IQGAP1, and WAVE2. B16F10 cells were double transfected with GFP-IQGAP1 and Myc-ΔGRD and were then stained with anti-Myc and anti-WAVE2 antibodies. The Myc-ΔGRD (red), GFP-IQGAP1 (green), and WAVE2 (blue) were combined and areas in retracting edges and protruding edges were enlarged.

We next looked at Myc-ΔCT which is missing the CT domain of IQGAP1 as well as the rest of the C-terminus. Upon examination of the localization of GFP-IQGAP1 and Myc-

ΔCT (Figure 15) we saw that Myc-ΔCT localized to WAVE2 positive areas of the cell and not to areas of retraction like GFP-IQGAP1 localization. These results indicate that the CT domain plays an important role in the localization of IQGAP1 to areas of retraction.

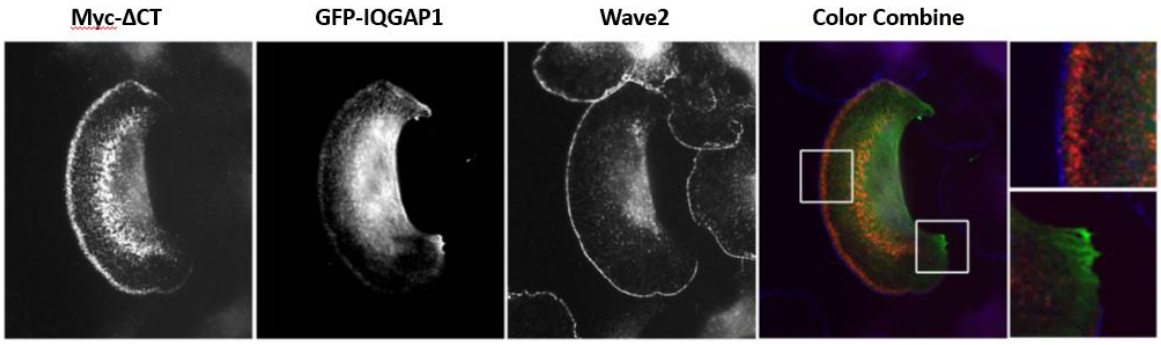

Figure 15. Subcellular localization of Myc-ΔCT, GFP-IQGAP1, and WAVE2. B16F10 cells were double transfected with GFP-IQGAP1 and Myc-ΔCT and were then stained with anti-Myc and anti-WAVE2 antibodies. The Myc-ΔCT (red), GFP-IQGAP1 (green), and WAVE2 (blue) were combined and areas in retracting edges and protruding edges were enlarged.

Analysis of Myc-Tagged IQGAP1 Mutants

When we decided to perform the double transfection of GFP-IQGAP1 and the Myc-tagged IQGAP1 mutants in the B16F10 cells, we quickly came to realize that we were going to have to find a way to validate that all of this IQGAP1 which was present in the cell was not completely saturating binding locations of IQGAP1. This is important due to the fact that there are three forms of IQGAP1 in the cell after the double transfection has been performed: the native IQGAP1 to the cell, the GFP-IQGAP1, and the Myc-IQGAP1. This means that the potential for saturation at the binding locations for IQGAP1 is a real possibility. With this in mind we decided to examine the retraction fluorescence of GFP-IQGAP1 to the whole cell fluorescence of GFP-IQGAP1 in the corresponding cell. The resulting graph is shown below in Figure 16. What we saw was that there was a direct correlation between the fluorescence values for areas of retraction and those for the whole cell. This demonstrated that as the total amount of GFP-IQGAP1 in the cell increased we saw an increased amount of

GFP-IQGAP1 in areas of retraction. This showed that the cells we were looking at were not saturated with IQGAP1 to the point that there was no binding location for the GFP-IQGAP1.

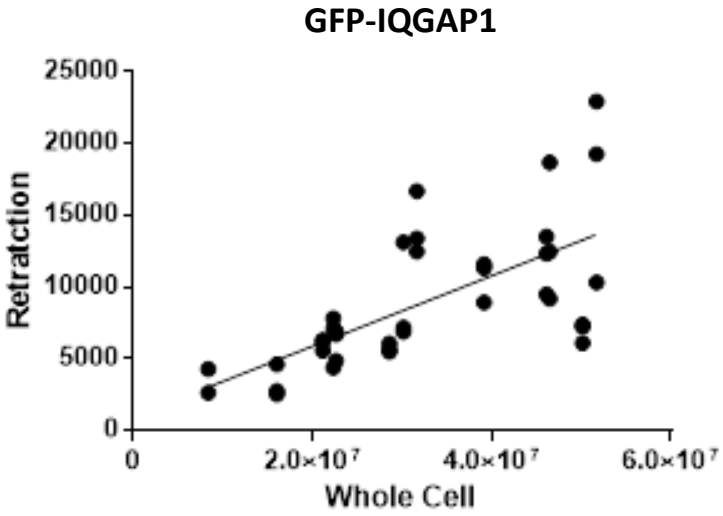

Figure 16. Correlation of GFP-IQGAP1 fluorescence retraction versus whole cell. GFP-IQGAP1 fluorescence values in areas of retraction were plotted against the whole cell GFP-IQGAP1 fluorescence values for the corresponding cell. The data shows that a direct correlation exists between retraction fluorescence values and whole cell fluorescence values for GFP-IQGAP1.

While we were ensuring that GFP-IQGAP1 in retracting areas had a direct correlation with the overall amount of GFP-IQGAP1 in the cell, we were also ensuring that there was a direct correlation between the amount of Myc-IQGAP1 in areas of retraction and the overall amount of Myc-IQGAP1 in the cell. We felt this was necessary due to the fact that the Myc-tag might interfere with the IQGAP1 localization causing it to have a lower affinity for the binding location than that of the GFP-IQGAP1. This could result in there not being a direct correlation between the Myc-IQGAP1 fluorescence in areas of retraction and the total Myc-IQGAP1 fluorescence in the cell. So like the GFP-IQGAP1, we plotted the fluorescence values for Myc-IQGAP1 in areas of retraction against the whole cell Myc-IQGAP1 values for corresponding cells. This can be seen below in Figure 17. We found that once again, like the GFP-IQGAP1, we had a direct correlation between the Myc-IQGAP1 fluorescence values

for areas of retraction and the Myc-IQGAP1 whole cell fluorescence values. Meaning that once again for the cells which we were investigating we were not saturating the binding site for IQGAP1.

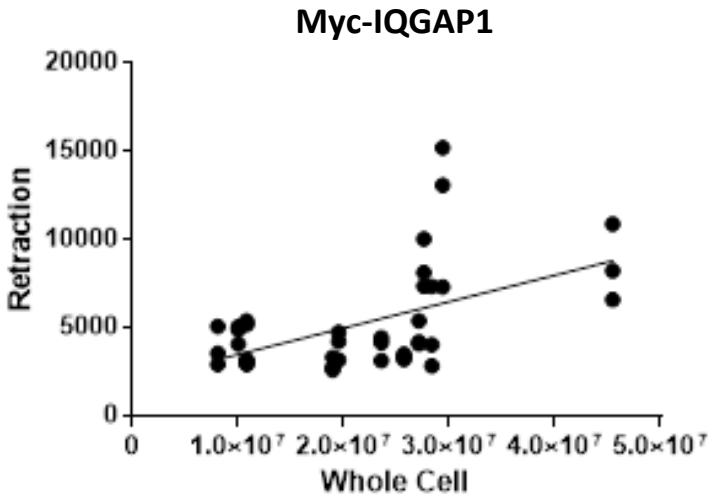

Figure 17. Correlation of Myc-IQGAP1 fluorescence retraction versus whole cell. Myc-IQGAP1 fluorescence values in areas of retraction were plotted against the whole cell Myc-IQGAP1 fluorescence values for the corresponding cell. The data shows that a direct correlation exists between retraction fluorescence values and whole cell fluorescence values for Myc-IQGAP1.

Once we had determined the validity of the fluorescence values for the Myc-IQGAP1 and GFP-IQGAP1 in areas of retraction we turned our attention to how we were going to analyze and present the data we had obtained with fluorescence microscopy. We knew that we could not directly compare the fluorescence values we obtained in one cell with those we obtained from a different cell. The reason behind this is, as we have already shown, the fluorescence in the area of localization for both the GFP-IQGAP1 and the Myc-IQGAP1 directly correlate to their respective whole cell value for fluorescence. While this means we could not directly compare the values to one another it did present us with a solution. We could take a ratio of the fluorescence values at areas of retraction and the whole cell values for fluorescence. We took the resulting ratio of the Myc-tagged IQGAP1 mutant and divided

it by the ratio of the GFP-IQGAP1, which was our wild type control, to get a ratio showing amount of fluorescence at areas of localization. This would allow us to compare values which were obtained from different cells, and therefore different levels of expression with one another. Equation 1 below shows the formula which was just described.

$$\frac{\dfrac{\text{Myc-Mutant Retraction Fluorescence}}{\text{Myc-Mutant Whole Cell Fluorescence}}}{\dfrac{\text{GFP-IQGAP1 Retraction Fluorescence}}{\text{GFP-IQGAP1 Whole Cell Fluorescence}}}$$

Formula 1. Formula used for the calculation of the ratio of ratios for retraction. This formula was used to obtain the values which were compiled to make Figure 18. This formula allowed for the correction of different expression levels of GFP-IQGAP1 and Myc-tagged IQGAP1 mutants in B16F10 cells.

The values generated by Formula 1 were then compiled and used to generate the bar graph seen in Figure 18. To determine the significance of the results which were seen in Figure 18 an unpaired t-test was performed which resulted in $p<0.015$ for Myc-ΔCHD and $p<0.0001$ for both Myc-ΔGRD and Myc-ΔCT. This data shows that there is a clear lack of both the Myc-ΔCT and Myc-ΔGRD at areas of retraction in B16F10 cells.

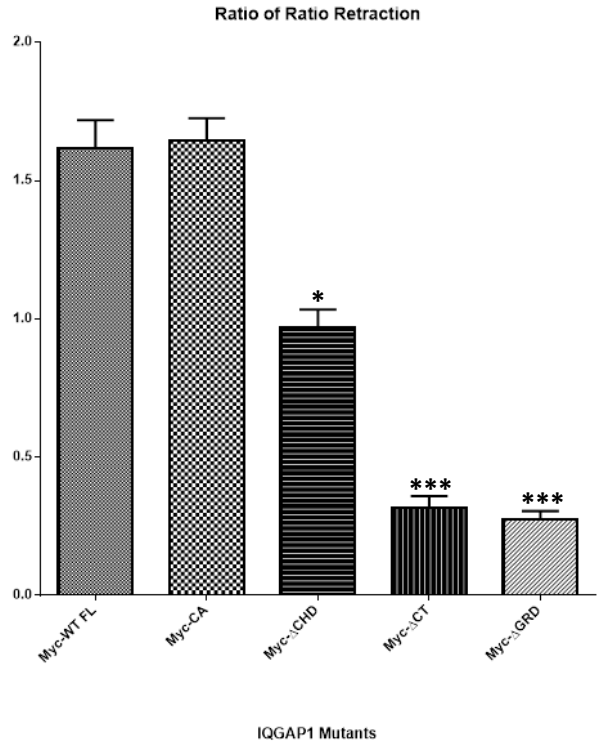

Figure 18. Ratio of ratio bar graph for retraction. This is a bar graph showing the average of the ratio of ratio calculation for each Myc-tagged mutant of IQGAP1 in areas of retraction.

Once we had obtained the fluorescence microscopy images for the Myc-ΔGRD and Myc-ΔCT we saw that in addition to analyzing the values we had obtained for areas of retraction it would also be necessary to analyze the images for areas of protrusion as well. With this thought in mind we decided to repeat the ratio of ratios method described previously but use the fluorescence values we had obtained at areas of protrusion in place of the fluorescence values for areas of retraction. Equation 2 below shows the formula which was used to calculate the ratio of ratios values used to generate the data compiled in Figure 19.

$$\frac{\dfrac{\text{Myc-Mutant Protrusion Fluorescence}}{\text{Myc-Mutant Whole Cell Fluorescence}}}{\dfrac{\text{GFP-IQGAP1 Protrusion Fluorescence}}{\text{GFP-IQGAP1 Whole Cell Fluorescence}}}$$

Formula 2. Formula used for the calculation of the ratio of ratios for protrusion. This formula was used to obtain the values which were compiled to make Figure 19. This formula allowed for the correction of different expression levels of GFP-IQGAP1 and Myc-tagged IQGAP1 mutants in B16F10 cells.

Figure 19 below shows the average for the ratio of ratios calculation for each Myc-tagged IQGAP1 mutant at areas of protrusion. To show the significance of the data an unpaired t-test was performed which resulted in $p<0.01$ for both Myc-ΔGRD and Myc-ΔCT. These results show us that there is clearly a much greater amount of both Myc-ΔGRD and Myc-ΔCT in areas of protrusion.

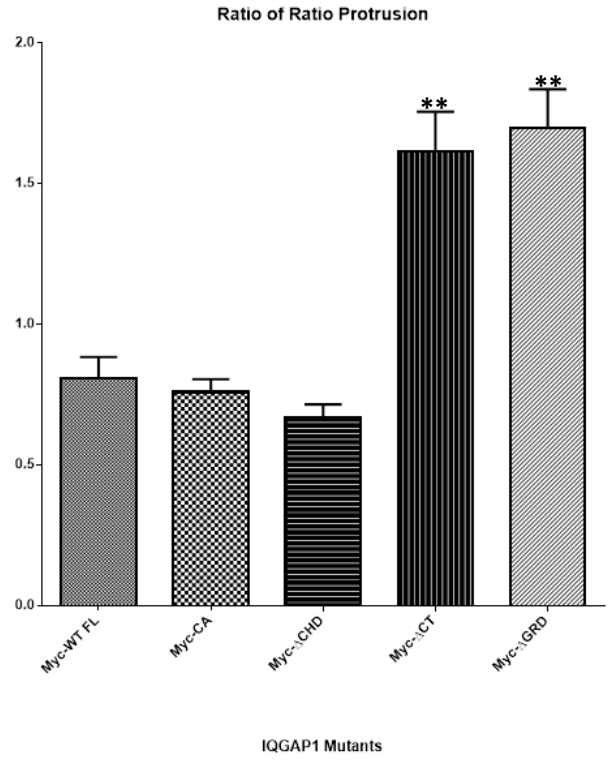

Figure 19. Ratio of ratio bar graph for protrusion. This is a bar graph showing the average of the ratio of ratio calculation for each Myc-tagged mutant of IQGAP1 in areas of protrusion.

Knockdown of IQGAP1 in B16F10 Cells

We have shown that IQGAP1 localizes to areas of retraction in the B16F10 cell line. With this in mind we set out to determine what would happen if we knockdown IQGAP1 in the cells. The experiment was performed by inserting a short hairpin RNA by means of the lentivirus. We also had two controls for the experiment, the first being a regular B16F10 cell and the second being a B16F10 cell which was subject to the lentivirus with no shRNA. The transfected and control cells were then placed on separate laminin coated coverslips and allowed to attach and spread for 30 minutes. They were then fixed and examined using fluorescence microscopy. What we see in Figure 20 is that both the control cell and virus control cell both form a broad lamellipodium with clear defined areas of retraction. What we see from the knockdown cell is no lamellipodium and retraction on all sides of the cell. While the results are preliminary and only actin images they validate a more thorough examination of the knockdown cells.

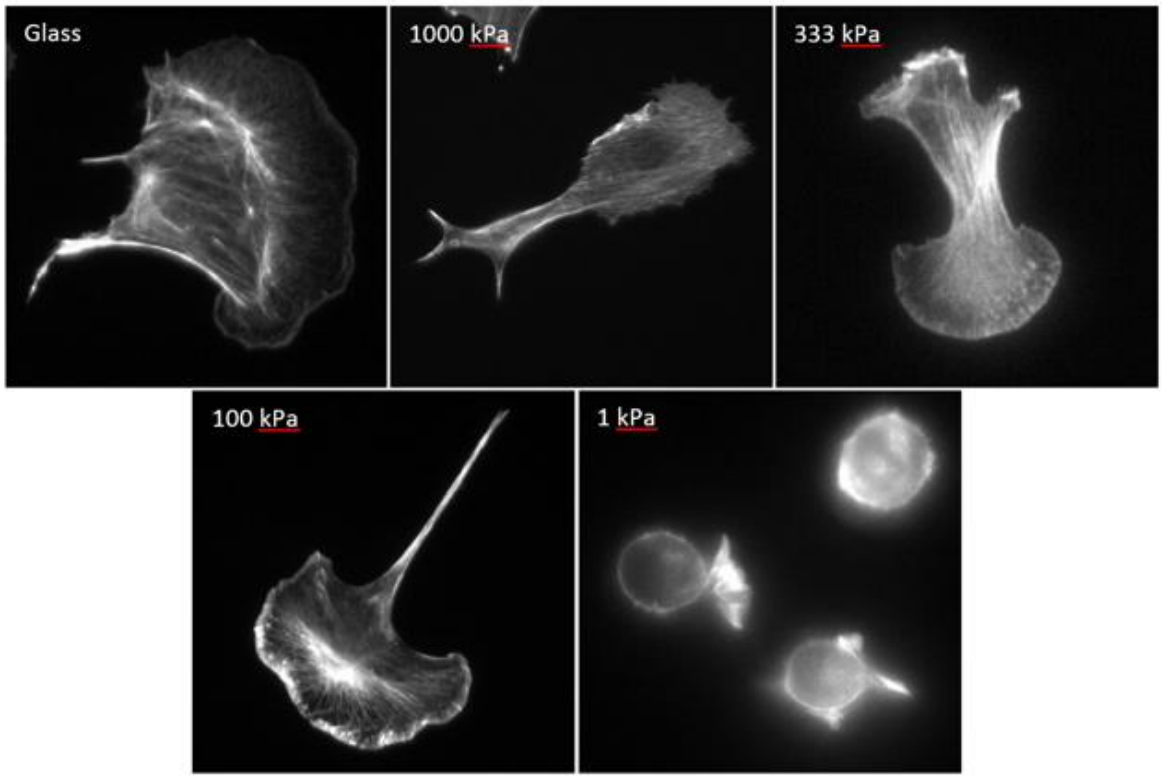

Figure 20. Actin image of B16F10 cells on various stiffness of hydrogels and glass. Cells were place on hydrogel surface and allowed to spread and move for 3 hours prior to image capture. They were then fixed and stained with phalloidin.

B16F10 Cell Response to Surface Stiffness

Previous studies have shown that cell response varies with the stiffness of the surface the cell is on [10]. With this knowledge in mind we decided to look at the effect of surface stiffness on the localization of IQGAP1. To perform this experiment we made hydrogels according to the protocol described previously. We then put regular B16F10 cells on the laminin coated hydrogels. What we see in Figure 21 is actin images of the cells after they have been allowed to spread and move on the laminin coated hydrogels for 3 hours. We can see in the glass, 1000 kPa, 333 kPa, and 100 kPa that the cells have a normal shape with a broad lamellipodium and areas of retraction. We also see that on the 1 kPa the cells do not spread at all. They are round and do not form a lamellipodium or areas of retraction.

Figure 21. Actin image of B16F10 control, virus control, and knockdown. Virus control cell was exposed to the lentivirus and the knockdown cell was exposed to the lentivirus with shRNA.

CHAPTER V

DISSCUSSION

Localization of Myc-Tagged IQGAP1 Mutants

It has been shown previously that IQGAP1 localizes to the leading edge of cells by numerous studies [3]. In our previous research we have shown that IQGAP1 does not always localize to the leading edge and that localization is cell type dependent. The study showed that IQGAP1 can localize to the leading edge or even retracting cell edges [11]. In our current study we explored IQGAP1 and Myc-tagged IQGAP1 mutants localization in B16F10 cells. We found that localization of IQGAP1 in B16F10 cells was very much dependent on the domains of IQGAP1. Using a double transfection of GFP-IQGAP1 and Myc-tagged mutants combined with immunofluorescence we were able to determine the localization of the mutants compared to wild type localization. In addition, the double transfection allowed for a ratiometric measurement to correct for differences in expression level. We saw that the Myc-WTFL localized to the same areas of retraction in the cell as the GFP-IQGAP1 which meant that neither the Myc-tag nor the GFP was interfering with the localization of IQGAP1. We then moved on and saw that the Myc-CA also localized to the same areas of retraction in the cell as GFP-IQGAP1. We saw that the Myc-ΔCHD localized to retracting areas, but also to the lamella behind protruding edges. We then saw that both Myc-ΔGRD and Myc-ΔCT localized to areas of protrusion. We took these results and decided to combine them with other models we had seen for IQGAP1 to make a new model (Figure 22).

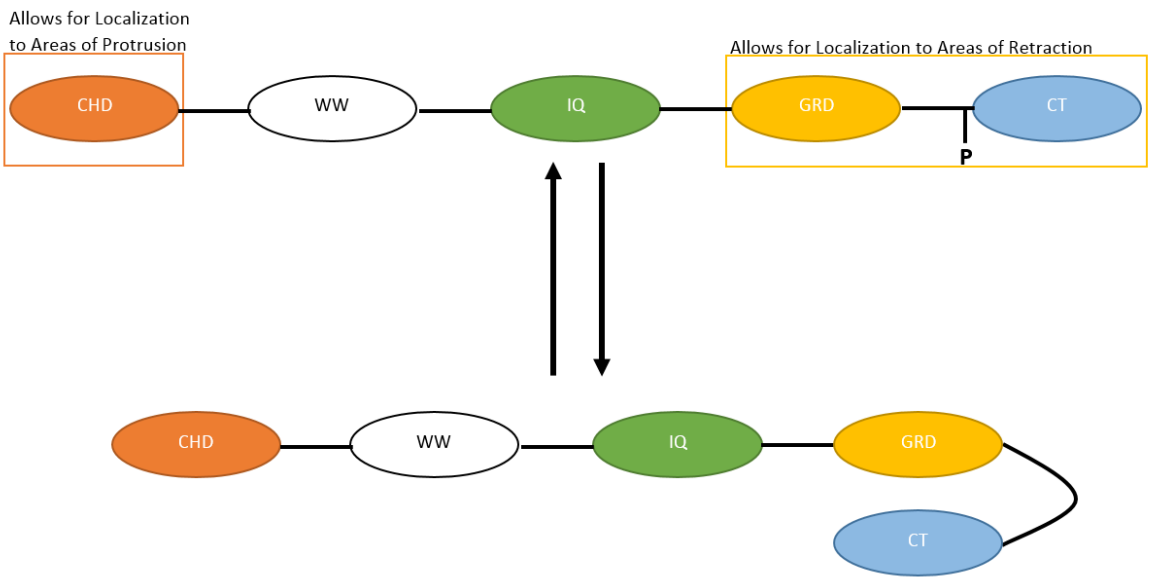

Figure 22. Model for IQGAP1 in B16F10 cells. Phosphorylation at serine 1443 causes the protein to be in what is known as the open configuration. When IQGAP1 is in this open conformation it is considered to be active. When the serine is dephosporylated it is considered to be inactive and in the closed conformation.

We know from our research that the GRD domain, CT domain, and phosphorylation of serine 1443 are important for localization of IQGAP1 to areas of retraction in B16F10 cells. This is shown by the fact that the loss of the GRD domain or CT domain results in IQGAP1 localizing to the protruding edge of cells. We also saw that the constitutively active localizes to areas of retraction meaning that the phosphorylation of the serine at 1443 is important. We also know that CHD is important for localization of IQGAP1 to areas of protrusion. This has been shown previously [12], and is also supported by our experiments which show a slight decrease in the localization to areas of protrusion when the CHD domain is removed. The CHD domain has been previously shown to interact with N-WASP [12]. We believe it is this interaction which is causing the CHD domain to be responsible for localization to areas of protrusion. Another study has showed us that the GRD domain is known to interact with CDC42 [4]. It is possible that this interaction with CDC42 and the

GRD domain is what is causing the localization of IQGAP1 to areas of retraction in B16F10 cells.

Knockdown of IQGAP1 in B16F10 Cells

Once we had found what domains are important to the localization of IQGAP1 we wanted to set out to determine what IQGAP1 did in the cell. To determine this we decided to perform a knockdown experiment on IQGAP1 in B16F10 cells. We accomplished this by the insertion of shRNA into the host genome by means of the lentivirus. We did this in order to specifically look at how cells are retracting, how they are protruding, what the general cell shape and area are, and eventually how the cells move. The results we showed about are just representative actin images of the cell which have not been analyzed yet. As we can see in the cell the control cell and virus control cell are normal looking cells which have broad lamellipodium and areas of retraction as we would expect in a cell that is moving. What we see in the knockdown cell however is quite interesting it has actually got no lamellipodium and as areas of retraction all the way around the perimeter of the cell. This gives us hope that we will be able to get more concrete information out of analysis of the images.

B16F10 Cell Response to Surface Stiffness

Numerous papers have shown that stiffness of the surface a cell is on can have various effects on the cell such as drug activity [13], cell morphology [10], and cell adhesion [10]. We decided to explore the effects of surface stiffness on the localization of IQGAP1. To do this we used polyacrylamide gels to mimic tissue stiffnesses. Surface stiffness based on the amount of polyacrylamide has been explored previously by other labs [10]. We made our polyacrylamide gels based on their procedures. We then placed cells on the various stiffnesses to observe the effects. As you see in the actin images that we obtained, the cell

shape for glass, 1000 kPa, 333 kPa, and 100 kPa are normal cells with broad lamellipodium and areas of retraction. As we can see in the 1 kPa image the cell is not spread out at all and it is spherical. All of the images were taken after three hours of spreading and moving. This means that if we went with a shorter time point we might see less spreading in the 1000 kPa, 333 kPa, and 100 kPa stiffness gels. We think that the cells on the 1 kPa gel don't spread due to the fact that the stiffness is not rigid enough for the cells to generate any force. B16F10 cells are, as previously mentioned, mouse melanoma cells. Melanoma is a type of skin cancer, and as you can see in Figure 23 the stiffness of skin can vary form 25 kPa to 100 kPa depending on what part of the body the is being discussed.

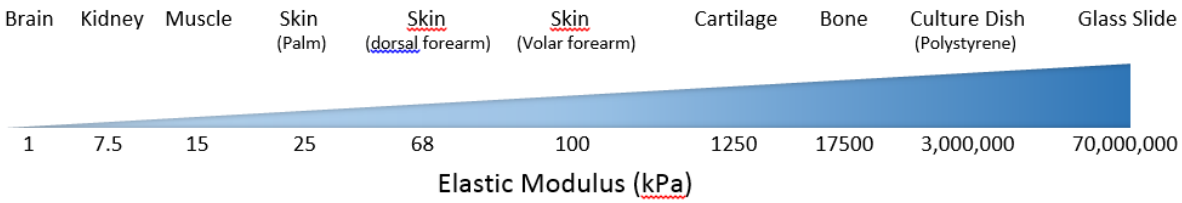

Figure 23. Stiffness of various tissues and materials. The stiffness of various tissues in the human body as well as the stiffness of common materials which cells are studied on. The stiffnesses were obtained by means of young's elastic modulus.

CHAPTER VI

FUTURE WORK

Analysis of IQGAP1 Knockdown Cell Line

Looking at the work which has been done far, there are some obvious future direction which can be taken to investigate IQGAP1 further. One of these future direction is to continue the investigation of the IQGAP1 knockdown cell line. So far we have obtained actin images of the knockdown cells, as well as both of the control cells. A more rigorous method of analysis which could be done is to look at various properties of the knockdown cells in comparison to both of the control cells. The properties which would be investigated would include shape factor, actin content, and spreading area. Investigation of these properties would be done by analysis of the existing or even future fluorescence microscopy images of stained actin in the knockdown, virus control, and control cells by means of metamorph software. Looking at these properties we would hopefully be able to identify possible roles of IQGAP1 in the cell. Based on the preliminary results which we have seen in the knockdown study we expect to see that the shape factor would result in a much more round cell. Additionally, we would expect to see that the knockdown cells would not spread out as much as the control cells. The actin content of the knockdown cell we would expect to be similar to that of the control cell.

IQGAP1 Localization on a Lower Stiffness

Another area which could be explored in greater detail is how IQGAP1 reacts in cells which are on a softer stiffness than that of glass. All of the IQGAP1 studies we have conducted to this point have been on glass and, as previously mentioned, it is well documented that cells behave much differently on glass than they do on softer surfaces.

Examples of this being drug activity [13], cell morphology [10], and cell adhesion [10]. As shown in Figure 23, skin cells are in the range of 25 to 100 kPa and glass is about 70,000,000 kPa. It would be interesting to see where IQGAP1 localizes on the much softer surface. The localization which is seen by this experiment would be much closer to physiological conditions for the B16F10 cells. The experiment would be conducted by repeating the previously mentioned process of creating the polyacrylamide hydrogels and placing B16F10 cells on the laminin coated surface of the gels. The cells would then be fixed and stained with an antibody for IQGAP1 and WAVE2 and images of the cells would be obtained by means of fluorescence microscopy. IQGAP1 localization would then be determined by looking at WAVE2 positive and negative areas to see if IQGAP1 localized to either of them. On the softer surfaces we hypothesize that we would not see IQGAP1 localize to any areas consistently. While on the stiffer surfaces, greater than 100 kPa, we would hypothesize that IQGAP1 would localize to areas of retraction in B16F10 cells.

Laminin Content Based on Gel Stiffness

One of the questions which presents itself when thinking about the effect surface stiffness has on the cell is what the appearance of the surface is. The cell is behaving much differently on the 1 kPa surface than it does on even the 100 kPa surface. The question we want to investigate more thoroughly is if the stiffness alone is responsible for the effect we are seeing on the cell or if there is some difference in the composition of the surface which is also having an effect. In order to investigate this question the first step would be to see if the laminin content of the various hydrogels is the same as each other as well as the glass. In order to perform this experiment the previously mentioned procedure would be followed to create the polyacrylamide hydrogels to the desired stiffness. They would then be cross-linked with Sulfo-SANPAH as previously described and laminin would be added at the

desired concentration. They would then be stained with an antibody for laminin and images would be taken by means of fluorescence microscopy. Analysis of the intensity of the fluorescence seen on the various stiffnesses would allow for the determination of the relative amount of laminin on each of them. This would show if the stiffness of a surface has an effect on the laminin content. We expect to see that the laminin content is not impacted by the stiffness of the surface to a significant margin. We believe that the laminin content will be independent of surface stiffness.

REFERENCES

1. Lauffenburger, D. A., Horwitz, A. F. Cell Migration: A Physically Integrated Molecular Process. *Cell.* **1996**, 84, 359-369.

2. Yamaguchi, H., Jeffrey W., and John C. Cell migration in tumors. *Current opinion in cell biology.* **2005**, 17(5), 559-564.

3. White, C. D., Erdemir, H. H., Sacks, D. B. IQGAP1 and Its Binding Proteins Control Diverse Biological Functions. *Cell Signal.* **2013**, 24(4), 826-834.

4. Fukata M., Kuroda S., Fujii K., Nakamura T., Shoji I., Matsuura Y., Okawa K., Iwamatsu A., Kikuchi A., Kaibuchi K. Regulation of cross linking of actin filament by IQGAP1, a target for Cdc42. *Journal of Biological Chemistry.* **1997**, 272, 29579–29583.

5. Le Clainche C., Schlaepfer D., Ferrari A., Klingauf M., Grohmanova K., Veligodskiy A., Didry D., Le D., Egile C., Carlier M. F., Kroschewski R. IQGAP1 stimulates actin assembly through the N-WASP-Arp2/3 pathway. *Journal of Biological Chemistry.* **2007**, 282, 426–435.

6. Fukata M., Watanabe T., Noritake J., Nakagawa M., Yamaga M., Kuroda S., Matsuura Y., Iwamatsu A., Perez F., Kaibuchi K. Rac1 and Cdc42 capture microtubules through IQGAP1 and CLIP-170. *Cell*. **2002**, 109, 873–885.

7. Watanabe T., Wang S., Noritake J., Sato K., Fukata M., Takefuji M., Nakagawa M., Izumi N., Akiyama T., Kaibuchi K. Interaction with IQGAP1 links APC to Rac1, Cdc42 and actin filaments during cell polarization and migration. *Devlopemental Cell*. **2004**, 7, 871–883.

8. Noritake J., Watanabe T., Sato K., Wang S., Kaibuchi K. IQGAP1: a key regulator of adhesion and migration. *Journal of Cell Science*. **2005**, 118, 2085–2092.

9. Bisi, S., Disanza, A., Malinverno, C., Frittoli, E., Palamidessi, A., & Scita, G. Membrane and actin dynamics interplay at lamellipodia leading edge. *Current opinion in cell biology*, **2013**, *25*(5), 565-573.

10. Yeung, T., Georges, P. C., Flanagan, L. A., Marg, B., Ortiz, M., Funaki, M., Zahir, N., Ming, W., Weaver, V., Janmey, P. A. Effects of substrate stiffness on cell morphology, cytoskeletal structure, and adhesion. *Cell motility and the cytoskeleton* **2005**, 60(1), 24-34.

11. Foroutannejad, S., Rohner, N., Reimer, M., Kwon, G., & Schober, J. M. A novel role for IQGAP1 protein in cell motility through cell retraction. *Biochemical and biophysical research communications*, **2014** *448*(1), 39-44.

12. Bensenor L. B., Kan H. M., Wang N., Wallrabe H., Davidson L. A., Cai Y., Schafer D. A., Bloom G. S. IQGAP1 regulates cell motility by linking growth factor signalling to actin assembly. *Journal of Cell Science,* **2007**, 120, 658–669.

13. Rehfeldt, F., Engler, A. J., Eckhardt, A., Ahmed, F., Discher, D. E. Cell responses to the mechanochemical microenvironment—implications for regenerative medicine and drug delivery. *Advanced drug delivery reviews,* **2007**, 59(13), 1329-1339.